International Journal of Nanomedicine

Dovepress
open access to scientific and medical research

Open Access Full Text Article

ORIGINAL RESEARCH

The Adjuvant of α-Galactosylceramide Presented by Gold Nanoparticles Enhances Antitumor Immune Responses of MUC1 Antigen-Based Tumor Vaccines

This article was published in the following Dove Press journal:
International Journal of Nanomedicine

Yonghui Liu[1]
Zhaoyu Wang[1]
Fan Yu[2]
Mingjing Li[1]
Haomiao Zhu[1]
Kun Wang[1]
Meng Meng[1]
Wei Zhao[1]

[1]State Key Laboratory of Medicinal Chemical Biology, College of Pharmacy and KLMDASR of Tianjin, Nankai University, Tianjin 300353, People's Republic of China; [2]College of Life Sciences, Nankai University, Tianjin 300071, People's Republic of China

Background: Therapeutic tumor vaccines are one of the most promising strategies and have attracted great attention in cancer treatment. However, most of them have shown unsatisfactory immunogenicity, there are still few available vaccines for clinical use. Therefore, there is an urgent demand to develop novel strategies to improve the immune efficacy of antitumor vaccines.

Purpose: This study aimed to develop novel adjuvants and carriers to enhance the immune effect of MUC1 glycopeptide antigen-based antitumor vaccines.

Methods: An antitumor vaccine was developed, in which MUC1 glycopeptide was used as tumor-associated antigen, α-GalCer served as an immune adjuvant and AuNPs was a multivalent carrier.

Results: Immunological evaluation results indicated that the constructed vaccines enabled a significant antibody response. FACS analysis and immunofluorescence assay showed that the induced antisera exhibited a specific binding with MUC1 positive MCF-7 cells. Moreover, the induced antibody can mediate CDC to kill MCF-7 cells. Besides stimulating B cells to produce MUC1-specific antibodies, the prepared vaccines also induced MUC1-specific CTLs in vitro. Furthermore, the vaccines significantly delayed tumor development in tumor-bearing mice model.

Conclusion: These results showed that the construction of vaccines by presenting α-GalCer adjuvant and an antigen on gold nanoparticles offers a potential strategy to improve the antitumor response in cancer immunotherapy.

Keywords: MUC1 glycopeptide, α-galactosylceramide, gold nanoparticle, antitumor vaccine

Introduction

In recent years, therapeutic tumor vaccines have attracted great attention in cancer treatment.[1] MUC1 is a transmembrane glycoprotein that is overexpressed in many tumor tissues such as breast, pancreas, kidney, ovary, lung, colon and stomach.[2,3] It contains many variable number tandem repeats (VNTR) of 20 amino acids (HGVTSAPDTRPAPGSTAPPA) in the extracellular domain.[4] Each VNTR has five latent *O*-linked glycosylation sites in threonine or serine residues. The aberrant glycosylated antigens are called tumor-associated carbohydrate antigens (TACAs), including Tn antigen, TF antigen, sialyl Tn and sialyl TF antigen.[5] The polypeptide

Correspondence: Meng Meng; Wei Zhao
State Key Laboratory of Medicinal Chemical Biology, College of Pharmacy and KLMDASR of Tianjin, Nankai University, No. 38 Tongyan Road, Haihe Education Park, Tianjin 300353, People's Republic of China
Tel/Fax +86 22-23507760
Email mengmeng@nankai.edu.cn; wzhao@nankai.edu.cn

submit your manuscript | www.dovepress.com
DovePress
http://doi.org/10.2147/IJN.S273883

backbone of MUC1 VNTR and different TACAs form the tumor-specific antigens.[6] To improve the antigenicity, researchers usually conjugated MUC1 VNTR glycopeptide antigens with various carrier proteins, including bovine serum albumin (BSA),[7] keyhole limpet hemocyanin (KLH)[8] and tetanus toxoid (TTX).[9] However, these carrier proteins could induce a strong immune response against themselves and suppress the immunity to the MUC1 antigen. For this concern, immunological adjuvants have been developed to prepare MUC1-based vaccines, such as the ligands of Toll-like receptors (for example, Pam_3CSK_4,[10] Pam_3CS,[11] CpG,[12] MALP2,[13] FSL-1,[14] LipidA),[15] and self-assembly peptides[16,17] etc. Although most of them have shown decent immunogenicity, there are still no therapeutic vaccines available for clinical application. As antitumour immunity of tumor vaccines is a complex, multi-component process, and the optimal combinations of antigens, adjuvants, delivery systems and routes of injection are not yet identified. Therefore, there is still an urgent need to develop novel adjuvants and delivery systems to improve the immunogenicity of MUC1-based vaccines.

Invariant natural killer T (iNKT) cells are a kind of T lymphocytes subtype that show the potential to modulate the immune responses against tumors and pathogens.[18–20] iNKT cells hold the properties of classical T cells and natural killer (NK) cells. While classical T cells were activated by the peptide ligands via major histocompatibility complex (MHC) class I and II molecules, iNKT cells would be activated by glycolipid ligands which were presented by MHC class I-like molecule, CD1d.[21,22] After being activated, iNKT cells secrete Th1-type cytokines (such as IFN-γ and IL-2) and Th2-type cytokines (such as IL-4, IL-5 and IL-13).[23] The most intensively studied glycolipid molecules are α-galactosylceramide (α-GalCer, also call KRN7000) and its derivatives.[24,25] It has been reported that α-GalCer has been used to develop vaccines by conjugating with antigen epitopes, such as carbohydrate antigens.[26–30] peptide antigens[31–33] and nicotine antigen.[34]

Gold nanoparticles (AuNPs) have been served as a nanocarrier for the multivalent presentation of tumor associate antigens.[35–41] They can be conveniently prepared and the particle size could be easily controlled. More importantly, they can encapsulate a high density of antigen than traditional carrier proteins.[5,37] Cameron and co-workers developed multicopy multivalent gold nanoparticles as latent cancer vaccines based on Tn carbohydrate antigen.[37] Barchi and co-workers constructed spherical gold nanoparticles based cancer vaccines consisting of MUC4 glycopeptide antigen and adjuvant peptide.[36] The co-delivery of antigen with adjuvant by nano-gold particle to antigen-presenting cells (APCs) has been proved to stimulate an enhanced immune response.[42]

In the study, we developed an antitumor vaccine of MUC1 glycopeptide and α-GalCer via a gold-nanoparticle delivery system, in which MUC1 glycopeptide was used as tumor-associated antigen, α-GalCer served as an immune adjuvant and AuNPs was a multivalent carrier. To the best of our knowledge, this is the first study to conjugate the adjuvant of α-GalCer on the surface of gold nanoparticle with an antigen to trigger the immune response. The conjugation of MUC1 glycopeptide and α-GalCer with gold nanoparticles was performed under gentle conditions, no requiring heat or highly hydrophobic solvent, which would guarantee the in vivo bioactivity of MUC1 glycopeptide and α-GalCer. The constructed vaccines elicited strong immune responses to delay tumor development in tumor-bearing mice. Overall, the prepared strategy of vaccines presented here will be very promising for the development of cancer vaccines.

Materials and Methods

Synthesis of 6-NH_2-α-GalCer

All reagents were commercially available and used directly. Reactions were detected by Thin Layer Chromatography (TLC) and monitored with 254 nm UV fluorescence or *p*-anisaldehyde solution. Column chromatography was used to separate the reaction product. ^1H and ^{13}C NMR spectra were carried out by a Bruker AV 400 MHz spectrometer at 400 MHz and 100 MHz, respectively. Signals are presented according to their chemical shift (δ in ppm) of $CDCl_3$ (^1H, 7.26 and ^{13}C, 77.16), CD_3OD (^1H, 3.31 and ^{13}C, 49.00), pyridine-d5 (^1H, 8.74, 7.58, 7.22 and ^{13}C, 150.35, 135.91, 123.87). Coupling constants are presented in hertz. HR-ESI-MS was carried out on a Varian QFT-ESI mass spectrometer. MALDI-TOF MS was carried out using DHB or CHCA as a matrix on Varian 7.0T FTMS equipment. The synthesis and characterization of 6-NH_2-α-GalCer were as follows.

Methyl 6-O-Trityl-α-D-Galactopyranoside (2)

The solution of 1-O-methyl-galactoside 1 (4.0 g, 20.6 mmol) in pyridine (60 mL) was added trityl chloride (8.75 g, 30.9 mmol) and the mixture was stirred at 90°C

for 12 h, after which the solvent was removed in vacuo. The crude product was purified by flash column chromatography on silica gel (DCM/MeOH = 35/1) to yield pyranoside 2 (8.27 g, 92%) as white solid.

^{1}H NMR (400 MHz, MeOD) δ 7.46–7.40 (m, 6H), 7.25 (t, *J* = 7.4 Hz, 6H), 7.20 (d, *J* = 7.2 Hz, 3H), 4.68 (d, *J* = 3.7 Hz, 1H), 3.77 (dd, *J* = 9.8, 5.0 Hz, 2H), 3.70 (dd, *J* = 10.1, 3.7 Hz, 1H), 3.63 (dd, *J* = 10.1, 3.2 Hz, 1H), 3.41 (s, 3H), 3.39–3.35 (m, 1H), 3.27 (dt, *J* = 3.0, 1.5 Hz, 2H), 3.20 (dd, *J* = 9.8, 4.7 Hz, 1H).

^{13}C NMR (101 MHz, MeOD) δ 145.53, 129.87, 128.79, 128.09, 101.37, 88.00, 71.54, 71.44, 71.09, 70.21, 64.94, 55.52.

HRMS (m/z): $[M+Na]^+$ calcd. for $C_{26}H_{28}NaO_6$ 459.1784; found 459.1782.

Methyl 2,3,4-Tri-O-Benzyl-6-O-Trityl-α-D-Galacto pyranoside (3)

To a solution of methyl 6-O-trityl-α/β-D-galactopyranoside 2 (8.2 g, 18.78 mmol) in DMF (80 mL) was added sodium hydride (60% in mineral oil, 2.254 g, 93.93 mmol) portionwise at 0°C. After 1 h, benzyl bromide (11.16 mL, 93.93 mmol) was added. The reaction mixture was left to stir for 12 h after which it was quenched by the addition of MeOH (15 mL). The solvent was removed in vacuo. Then, the mixture was diluted with DCM, washed with water (3 x 100 mL) and brine, dried over Na_2SO_4. The crude product was purified by flash column chromatography (petroleum ether/ethyl acetate=20:1) to yield the benzyl ether 3 (11.95 g) as a white solid which was used in the next step without further purification.

Methyl 2,3,4-Tri-O-Benzyl-α-D-Galactopyranoside (4)

The solution of methyl 2,3,4-tri-O-benzyl-6-O-trityl-α-D-galactopyranoside 3 (11.94 g, 16.89 mmol) in CH_2Cl_2 (40 mL) and MeOH (80 mL) was added p-toluenesulfonic monohydrate (342 mg, 1.8 mmol) under argon. The mixture was quenched after 4 hours with triethylamine (0.5 mL). The solvent was removed in vacuo. Then, the mixture was diluted with DCM and washed with water (2 x 100 mL), saturated aq. $NaHCO_3$ solution and brine and dried over Na_2SO_4. The crude product was purified by column chromatography (petroleum ether/ethyl acetate = 5/1) to give 4 (7.53 g, 86% over two steps) as a light yellow solid.

^{1}H NMR (400 MHz, $CDCl_3$) δ 7.45–7.27 (m, 15H), 4.98 (d, *J* = 11.6 Hz, 1H), 4.90 (d, *J* = 11.7 Hz, 1H), 4.85 (d, *J* = 12.1 Hz, 1H), 4.76 (d, *J* = 11.8 Hz, 1H), 4.73–4.68 (m, 2H), 4.65 (d, *J* = 11.6 Hz, 1H), 4.06 (dd, *J* = 10.0, 3.4 Hz, 1H), 3.95 (dd, *J* = 10.1, 2.3 Hz, 1H), 3.88 (m, 1H), 3.76–3.68 (m, 2H), 3.48 (dt, *J* = 15.0, 7.6 Hz, 1H), 3.37 (s, 3H).

^{13}C NMR (101 MHz, $CDCl_3$) δ 138.84, 138.55, 138.27, 128.75, 128.63, 128.59, 128.51, 128.24, 128.15, 127.90, 127.77, 127.71, 98.96, 79.25, 76.59, 75.16, 74.56, 73.77, 73.74, 70.33, 62.53, 55.50.

HRMS (m/z): $[M+Na]^+$ calcd. for $C_{28}H_{32}NaO_6$ 487.2091; found 487.2095.

2-(2-(2-Azidoethoxy)ethoxy)ethyl 4-Methylbenzene sulfonate (6)

Compound 5 (1.2 g, 6.8 mmol) dissolved in pyridine (30 mL) followed by adding 4-methylbenzene-1-sulfonyl chloride (1.56 g, 8.2 mmol). The reaction was stirred for about 6 h until TLC showed that the reaction was completed, remove the solvent in vacuo. The crude product was purified by column chromatography (petroleum ether/ethyl acetate = 2/1) to give 6 (1.9 g, 85%).

^{1}H NMR (400 MHz, $CDCl_3$) δ = 7.79 (d, *J*=8.4, 2H), 7.35 (d, *J*=8.0, 2H), 4.15 (t, *J*=4.8, 2H), 3.69 (t, *J*=4.8, 2H), 3.63 (t, *J*=4.8, 2H), 3.59 (m, 4H), 3.35 (t, *J*=4.8, 2H), 2.44 (m, 3H).

^{13}C NMR (101 MHz, $CDCl_3$) δ = 144.81, 132.77, 129.77, 127.82, 70.52, 69.93, 69.25, 68.59, 50.51, 21.51.

HRMS (m/z): $[M+Na]^+$ calcd. for $C_{13}H_{19}N_3NaO_5S$ 352.0943; found 352.0942.

Methyl 6-(O-Diethylene-Glycol-2-Azidoethyl)-2,3,4-Tri-O-Benzyl-α-D-Galacto Pyranose (7)

The solution of methyl 2,3,4-tri-O-benzyl-α-D-galactopyranoside 4 (7.5 g, 16.14 mmol) in DMF (60 mL) was added sodium hydride (60% in mineral oil, 1.25 g, 32.28 mmol) at 0°C. After 0.5 h, the mixture was warmed to room temperature. Then, 2-(2-(2-azidoethoxy)ethoxy)ethyl 4-methylbenzenesulfonate 6 (10.6 g, 32.28 mmol) was added and the reaction mixture was stirred at r.t. for a further 4 h, after which the mixture was quenched by the addition of MeOH (10 mL). The solvent was removed in vacuo. Then, the mixture was diluted with DCM and washed with water (3 x 150 mL) and brine and dried over Na_2SO_4. The crude product was purified by column chromatography (petroleum ether/ethyl acetate = 4/1) to yield 7 (7.23 g, 72%) as a light yellow oil.

^{1}H NMR (400 MHz, $CDCl_3$) δ 7.41–7.22 (m, 15H), 4.95 (d, *J* = 11.5 Hz, 1H), 4.83 (dd, *J* = 11.9, 8.1 Hz, 2H), 4.73 (d, *J* = 11.8 Hz, 1H), 4.67 (m, 2H), 4.62 (d, *J* = 11.5 Hz, 1H), 4.03 (m, 1H), 3.96–3.91 (m, 2H), 3.88 (t, *J* = 6.4

Hz, 1H), 3.63–3.59 (m, 6H), 3.57 (m, 3H), 3.54–3.44 (m, 3H), 3.36 (s, 3H), 3.34–3.30 (m, 2H).

^{13}C NMR (101 MHz, $CDCl_3$) δ 138.87, 138.72, 138.55, 128.40, 128.35, 128.25, 128.12, 127.70, 127.61, 127.50, 98.79, 79.10, 76.49, 75.06, 74.70, 73.57, 73.29, 70.79, 70.71, 70.64, 70.58, 70.06, 69.91, 69.15, 55.35, 50.64.

HRMS (m/z): $[M+Na]^+$ calcd. for $C_{34}H_{43}N_3NaO_8$ 644.2942; found 644.2948.

6-(O-Diethylene-Glycol-2-Azidoethyl)-2,3,4-Tri-O-Benzyl-α/β-D-Galactopyranose (8)

Compound 7 (7.2 g, 11.58 mmol) was dissolved in glacial acetic acid (104 mL) and 0.5 M sulfuric acid (13 mL), and the mixture was heated to 100°C. After 4 h, the mixture was cooled to room temperature. Then, the mixture was diluted with DCM and neutralized with saturated aq. $NaHCO_3$ solution. Then, it was washed with water and brine, dried over Na_2SO_4. The crude product was purified by flash column chromatography (petroleum ether/ethyl acetate = 2/1) to give 8 (4.79 g) as a colorless oil which was used in the next step without further purification.

6-(O-Diethylene-Glycol-2-Azidoethyl)-2,3,4-Tri-O-Benzyl-α/β-D-Galactopyranosyl N-Trichloroacetimidate (9)

To the mixture of 8 (4.78 g, 7.87 mmol) and trichloroacetonitrile (3.84 mL, 37.92 mmol) in anhydrous DCM (40 mL) at 0°C was added DBU (120 μL). After 3 h, the solvent was removed in vacuo. The crude product was purified by flash column chromatography (petroleum ether/ethyl acetate/trimethylamine = 700/100/0.1) to give 9 (5.03 g) as a light yellow oil which was used in the next step without further purification.

(2S,3S,4R)-3,4-Bis-Tert-Butyldimethylsilyloxy-2-Hexacosanoylamino-1-(6-O-Diethylene-Glycol-2-Azidoethyl)-2,3,4-Tri-O-Benzyl)-α-D-Galactopyranosyl) Octadecane (11)

After the mixture of 9 (5.02 g, 6.67 mmol), 10 (4.12 g, 4.45 mmol) and 4 Å MS (5.0 g) in dry THF (12 mL) and Et_2O (60 mL) was stirred at r.t. for 0.5 h, the solution was cooled to −20°C, and then BF_3 Et_2O (1.2 mL) was added dropwise. The reaction mixture was stirred at −20°C for 6 h. Molecular sieves were filtered off through a Celite pat and washed with CH_2Cl_2 (25 mL). The filtrate and washings were combined and washed with saturated aq. $NaHCO_3$ solution and brine, dried over Na_2SO_4 and condensed in vacuum. The residue was purified by column chromatography (petroleum ether/ethyl acetate = 8/1) to give 11 (4.31 g, 37% over three steps) as a colorless oil.

^{1}H NMR (400 MHz, $CDCl_3$) δ 7.38–7.28 (m, 15H), 6.03 (d, J = 7.0 Hz, 1H), 4.94 (d, J = 11.4 Hz, 1H), 4.84 (d, J = 3.6 Hz, 1H), 4.80 (d, J = 11.6 Hz, 1H), 4.75 (d, J = 9.2 Hz, 1H), 4.69 (d, J = 11.2 Hz, 1H), 4.64 (m, 1H), 4.09 (m, 1H), 4.04 (dd, J = 10.1, 3.5 Hz, 1H), 3.99 (m, 1H), 3.98–3.85 (m, 5H), 3.79 (dd, J = 10.7, 8.3 Hz, 1H), 3.66–3.61 (m, 8H), 3.60–3.57 (m, 3H), 3.56–3.45 (m, 3H), 3.37–3.31 (m, 2H), 1.99 (t, J = 7.6 Hz, 2H), 1.54–1.43 (m, 6H), 1.26–1.23 (m, 66H), 0.90 (s, 9H), 0.89 (s, 9H), 0.87 (d, J = 7.1 Hz, 6H), 0.07 (s, 4H), 0.06 (s, 3H), 0.04 (s, 3H), 0.03 (s, 3H).

^{13}C NMR (101 MHz, $CDCl_3$) δ 173.35, 138.90, 138.82, 138.68, 128.48, 128.45, 128.34, 128.31, 127.94, 127.77, 127.65, 127.60, 127.46, 100.19, 79.14, 77.36, 76.64, 75.93, 75.79, 74.90, 74.87, 73.60, 72.92, 70.82, 70.77, 70.73, 70.61, 70.19, 69.73, 69.51, 69.22, 51.85, 50.74, 36.85, 33.43, 32.06, 30.06, 29.84, 29.72, 29.62, 29.61, 29.50, 26.27, 26.22, 25.77, 22.83, 18.46, 18.31, 14.26, −3.54, −3.74, −4.50, −4.80.

HRMS (m/z): $[M+Na]^+$ calcd. for $C_{89}H_{156}N_4NaO_{11}Si_2$ 1536.1201; found 1536.1205.

(2S,3S,4R)-2-Hexacosanoylamino-1-(6-O-Diethylene-Glycol-2-Azidoethyl)-2,3,4-Tri-O-Benzyl-α-Dgalacto pyranosyl) Octadecane-3,4-Diol (12)

The solution of TBAF (1 M in THF, 11.36 mL, 11.36 mmol) was added slowly to a solution of bis-TBS ether 11 (4.3 g, 2.84 mmol) in THF (40 mL). After 2.5 h, the reaction mixture was diluted with CH_2Cl_2 (150 mL). Solvents were removed in vacuo and the crude product was purified by silica column chromatography (petroleum ether/ethyl acetate = 3/1) to give 12 (3.25 g, 89%) as white waxy solid.

^{1}H NMR (400 MHz, $CDCl_3$) δ 7.38–7.28 (m, 15H), 6.42 (d, J = 8.5 Hz, 1H), 4.93 (d, J = 11.5 Hz, 1H), 4.88 (d, J = 11.6 Hz, 1H), 4.84 (d, J = 3.7 Hz, 1H), 4.77 (s, 2H), 4.68 (d, J = 11.6 Hz, 1H), 4.62 (d, J = 11.5 Hz, 1H), 4.23 (dd, J = 8.0, 3.2 Hz, 1H), 4.04 (dd, J = 10.0, 3.7 Hz, 1H), 3.98 (d, J = 1.5 Hz, 1H), 3.92–3.84 (m, 4H), 3.65–3.56 (m, 10H), 3.52–3.44 (m, 5H), 3.37–3.32 (m, 2H), 2.16 (m, 2H), 1.66–1.35 (m, 6H), 1.25 (m, 66H), 0.88 (t, J = 6.8 Hz, 6H).

^{13}C NMR (101 MHz, $CDCl_3$) δ 173.18, 138.59, 138.46, 137.94, 128.60, 128.56, 128.40, 128.25, 128.10, 127.82, 127.76, 127.55, 99.40, 79.39, 77.36, 76.30, 76.11, 74.84, 74.43, 74.36, 73.32, 72.82, 70.80, 70.68, 70.56,

70.17, 69.93, 69.82, 50.73, 49.50, 36.88, 33.30, 32.05, 29.83, 29.79, 29.69, 29.56, 29.49, 26.07, 25.85, 22.82, 14.26.

HRMS (m/z): $[M+Na]^+$ calcd. for $C_{77}H_{128}N_4NaO_{11}^+$ 1307.9472; found 1307.9475.

(2S,3S,4R)-1-(6-O-Diethylene-Glycol-2-Azidoethyl)-α-D-Galactopyranosyl)-2-Hexacosanoylaminooctadecane-3,4-Diol (6-NH_2-α-GalCer, 13)

The compound 12 (80 mg, 0.06 mmol) was mixed with Pd $(OH)_2$/C (20% w/w, wet 60 mg) in EtOH/chloroform (4/1, 2.5 mL), and the mixture was shaken under an H_2 atmosphere at 60 psi for 12 h. The catalyst was removed by filtration through a Celite pad and the pad was washed with a mixture of CH_2Cl_2/MeOH (4/1). The combined filtrate was concentrated under vacuum and the product was purified by silica flash column chromatography on silica gel (CH_2Cl_2/MeOH = 10/1) to afford the product 13 (49.3 mg, 83%) as a white solid.

^{1}H NMR (400 MHz, Pyr) δ 8.93 (d, *J* = 8.5 Hz, 1H), 5.52 (d, *J* = 3.2 Hz, 1H), 5.17 (d, *J* = 4.1 Hz, 1H), 4.60 (m, 3H), 4.43–4.30 (m, 5H), 4.00 (t, *J* = 5.4 Hz, 2H), 3.93 (t, *J* = 4.8 Hz, 2H), 3.68 (d, *J* = 3.8 Hz, 2H), 3.60 (m, 6H), 3.53–3.47 (m, 2H), 2.57 (m, 2H).1.90–1.50 (m, 6H), 1.25 (m, 66H), 0.88 (t, *J* = 6.8 Hz, 6H).

^{13}C NMR (101 MHz, Pyr) δ 173.51, 100.90, 76.20, 72.46, 71.30, 71.08, 70.92, 70.79, 70.61, 70.58, 70.41, 70.28, 69.83, 68.14, 67.58, 67.56,51.23, 39.92, 36.79, 34.06, 32.14, 32.13, 30.43, 30.20, 30.07, 30.02, 29.99, 29.96, 29.93, 29.82, 29.65, 29.62, 26.55, 26.47, 22.95.14.30.

HRMS (m/z): $[M+Na]^+$ calcd. for $C_{56}H_{112}N_2NaO_{11}$ 1011.8158; found 1011.8162.

Synthesis of MUC1(Tn) Glycopeptide

MUC1 glycopeptide was synthesized on account of the standard Solid Phase Peptide Synthesis (SPPS) procedure. The peptide synthesis was conducted with natural Fmoc amino acids using HBTU (4.0 equiv), HOBt (4.0 equiv), DIPEA (8.0 equiv). Fmoc O-glycosylated amino acid and Fmoc-Pam_2Cys-OH were introduced using more reactive HATU (2.0 equiv), HOAt (2.0 equiv), DIPEA (4.0 equiv). The acetyl moieties of the Tn antigen were moved out through MeONa/MeOH (pH = 10~11). All acid-sensitive side-chain-protecting groups were moved out and the (glycolipo)peptides were detached from the resin through 90% TFA, 5% TIPS, 5% H_2O. The semi-preparative HPLC was employed to separate and purify the crude product on a C18 column (10×250 mm). UV absorption signals were monitored with a UV detector at 220 nm.

Purity Assessment

The biologically tested glycopeptide MUC1(Tn) possessed a purity of 99.9%, which was assessed by reverse phase HPLC and mass spectrometric analysis. The synthetic glycolipid α-GalCer was highly pure by analyzing ^{1}H NMR spectroscopy.

Synthesis of AuNPs Vaccines

AuNP-a and AuNP-b with a diameter of 4.9 ± 0.4 nm were synthesized according to a literature procedure.[43]

MUC1(Tn) and 6-NH_2-α-GalCer were coupled to N-hydroxysuccinimide-11-mercaptoun -decanoate (MUDHSE) coordinated AuNP (AuNP-b) accordingly to a previously reported procedure,[43] with minor modifications. Shortly, for the preparation of AuNP-1, 0.2 μM solution of MUDHSE coordinated AuNP (AuNP-b) in 4 mL of DMF was added to the solution of MUC1(Tn) (1.78 mg, 0.8 μmol) and 6-NH_2-α-GalCer (0.39 mg, 0.4 μmol). The solution was stirred for 0.5 h followed by adding a drop of trimethylamine. The solution was stirred overnight then dialyzed 3 times by DMF (200 mL) and triple-distilled water (200 mL). The AuNPs stock solution was then diluted to be 100 nM. For the preparation of AuNP-2, the solution of MUC1(Tn) (1.78 mg, 0.8 μmol) and 6-NH_2-α-GalCer (0.79 mg, 0.8 μmol) were employed. For AuNP-3 solution preparation, MUC1(Tn) (1.78 mg, 0.8 μmol) and 6-NH_2-α-GalCer (1.58 mg, 1.6 μmol) were used.

TEM Measurement

AuNPs in PBS solution were prepared, and each sample (3 μL) was dropped to copper grids with carbon-coated support films. The excess solution was removed with filter paper and the copper grid was washed twice with double-distilled water. The grids were allowed to dry in air overnight, and then imaged with JEM100CXII system at 100 kV.

DLS and Zeta Potential

DLS measurements were acquired using a Malvern Panalytical Zetasizer Nano ZSP. Samples were passed through a syringe filter (0.22 μm) prior to analysis.

Generation of BMDCs and in vitro Activation of BMDCs

BMDCs were first prepared. Balb/c mice were used to collect bone marrow cells through flushing the tibias and

femurs with 15 mL of cold DMEM. The cells were washed and re-suspended in the following medium: IMDM supplemented with 10% FBS, 100 U/mL penicillin, 100 μg/mL streptomycin, 50 μM β-mercaptoethanol supplemented with 10 ng/mL mouse IL-4 (Thermo Scientific) and 20 ng/mL mouse GM-CSF (Thermo Scientific). Seven days later, BMDC were harvested for the following measurement. BMDCs (2×10^5 cells/mL) were treated with PBS, α-GalCer+MUC1, AuNP-1, AuNP-2 or AuNP-3 for 18 h. The concentrations of IL-6 and IL-12 were measured with the ELISA Kits (Biolegend).

Mice and Immunological Studies

Female Balb/c mice (6–8 weeks, 6 mice/group) were employed for the immune evaluation. Mice were vaccinated subcutaneously biweekly with AuNP-1, AuNP-2 and AuNP-3, which contained approximately 20 μg MUC1 glycopeptide per dose, or with MUC1(Tn) and α-GalCer mixture (20 μg in 100 μL PBS) for four times. One week after the fourth immunization, sera and spleens were collected for immune evaluation. This study was approved by the Animal Ethical and Welfare Committee of the Institute of Radiation Medicine, Chinese Academy of Medical Sciences and conducted in accordance with the principles of the Institutional Animal Care and Use Committee. The approval number of animal ethics and welfare is IRM-DWLL-2,018,018.

Analysis of Antibody Titers

High-binding 96-Well ELISA plates were enveloped with MUC1 glycopeptide HGVTSAPDT(α-GalNAc) RPAPGSTAPPA (20 μg/mL) in a coating buffer and incubated 12 h at 4°C. The plates were washed with PBST buffer (0.1% Tween-20 in PBS) three times. Then, the plates were blocked by 1% BSA in PBST buffer. After blocking, the mouse sera diluted with 1% BSA in PBST were added at the presupposed diluted concentration and incubated 2 h. The plates were washed three times and incubated with horseradish peroxidase-conjugated goat anti-mouse IgG (diluted with 1:5000) for 1 h. The plates were then washed five times and TMB substrate was added. H_2SO_4 (0.5 M) solution was added to quench the reaction 30 min later. The absorbance at 450 nm was measured. Antibody titers were defined as the largest dilution times of the sera with 0.1 or higher optical density than the blank sera.

Analysis of Antibody Isotypes

To analyze the antigen-specific antibody isotypes, the Mouse Monoclonal Antibody Isotyping kit (Sigma-Aldrich, USA) was used. The measurement was conducted on the basis of the kit manual. Briefly, MUC1 glycopeptide HGVTSAPDT(α-GalNAc)RPAPGSTAPPA (20 μg/mL) was coated on the 96-well plates and blocked by 1% BSA in PBST before incubating the gradient diluted corresponding antisera. The goat anti-mouse isotype antibodies (IgG1, IgG2a, IgG2b, IgG3) with the dilution of 1/2000 were then added and rabbit anti-goat HRP-labeled secondary antibody was then added. TMB substrate solution (Thermo, USA) was added and H_2SO_4 (0.5 M) solution was then added to terminated the reaction. The plates were then analyzed at 450 nm by a microplate reader.

The Binding of Sera to MCF-7 and SK-MEL-28 Cells

MUC1 expressing MCF-7 cell and negative control of SK-MEL-28 cell (pursed from China Infrastructure of Cell Line Resource) were cultured in RPMI 1640 culture medium containing 10% FBS at 37°C. The cells were digested and washed with PBS solution for three times. The cells suspensions 5×10^5 per Eppendorf tube were incubated with 100 μL antiserum (1:50 dilution). The cells were incubated with FITC-conjugated rabbit anti-mouse IgG antibody (1:1000 dilution) after washing with PBS containing FBS (1%). The cells were then suspended in washing buffer (1 mL) and passed through a 200-mesh sieve, followed by detection on BD FACSAria III flow cytometry.

Immunofluorescence Staining

MCF-7 cell and SK-MEL-28 cell were cultured in 24-well plates. The cells were then fixed with 4% paraformaldehyde buffer at room temperature for 30 min. The fixed cells were washed with PBS and incubated with the antisera (1:50 dilution) at 4°C overnight. After washing with PBS, the cells were incubated with FITC-labeled goat anti-mouse IgG (1:100 dilution) for 30 min. The plates were then stained with 4′,6-diamidino-2-phenylindole (DAPI). Photographs were obtained with a laser scanning confocal microscope (Leica, Wetzlar, Germany).

Complement-Dependent Cytotoxicity (CDC) Assay

MCF-7 cells or SK-MEL-28 cells suspension (100 μL each well) were planked into a 96-well cell plate and

cultured overnight. Following by adding antisera (diluted 10 times with culture medium, 50 μL per well). Rabbit complement (Cedarlane, diluted 2 times with culture medium, 50 μL per well) was then added. The cells were then cultured for 12 h following by adding CCK-8 solution (Dojindo, 10 μL per well). The optical absorption at the wavelength of 450 nm was then measured 2 h later. The experiment was repeated three times. Cells adding CCK-8 only were used as control. The cytotoxicity was calculated based on the following formula.

Cytotoxicity (%) = [control OD – experimental OD)/ control OD] × 100%

Cytokines Analysis

One week after the fourth immunization, the spleens of mice in different groups were isolated followed by pressing the spleen through the stainless steel mesh sieve (80 μm) to obtain splenocytes. Then, splenocytes were washed twice with RPMI 1640 (10% FBS). Red blood cell lysis buffer was added following by washing twice. Splenocytes (1×10^6 cells per well) were seeded on 24-well culture plates in the presence of a growth medium containing MUC1 glycopeptide (10 μg/mL). After 2 days, the cell culture medium was collected and the levels of IL-4 and IFN-γ were measured with their ELISA Kits (BD Biosciences). Cytokine concentrations were calculated from standard curves.

Analysis of the Ratio of $CD8^+$ T Cells in Spleens and Tumors

Female Balb/c mice were immunized with the vaccine candidates four times. One week later, the spleens were isolated and splenocytes were collected. The cells were then stained with APC anti-mouse CD3e (Biolegend) and PE anti-mouse CD8a (Biolegend). The cells were washed three times and re-suspended in 500 μL FACS buffer for analysis using a BD LSR Fortessa flow cytometer and data were processed in Flow Jo software.

The ratio of tumor-infiltrating lymphocytes (TILs) were also tested. Briefly, tumor tissues were isolated and cut into pieces. The pieces were filtered through 70 μm mesh. The cells were then centrifuged and washed three times. Subsequently, the cells were stained with APC anti-mouse CD3e (Biolegend) and PE anti-mouse CD8a (Biolegend). The cells were washed three times and re-suspended in 500 μL FACS buffer for analysis using a BD LSR Fortessa flow cytometer and data were processed in Flow Jo software.

CTL Assay

CTL-mediated cytotoxicity in vitro was tested by Pierce LDH Cytotoxicity Assay Kit (Thermo Scientific). The experiment was carried out as described in the manual. The spleens were harvested from the mice immunized with the vaccine candidates. Then, splenocytes (Effector Cells) were isolated and added to 1×10^5 MCF-7 cells or SK-MEL-28 cells (Target Cells) with a ratio of 50:1. The viabilities of the tumor cells were evaluated by measuring the absorbance at 490 nm and 680 nm. To analyze LDH activity, the 680 nm absorbance value (background signal) was subtracted from the 490 nm absorbance.

% Cytotoxicity = [(Experimental value – Effector Cells Spontaneous Control – Target Cells Spontaneous Control)/ (Target Cell Maximum Control – Target Cells Spontaneous Control)] × 100%

Tumor Growth Inhibition

Female C57BL/6 Mice (4–6 weeks old) subcutaneously received MUC1 expressing B16-MUC1 tumor cells (1×10^5) in the right flank on day 0. The AuNPs-based vaccines AuNP-1, AuNP-2, AuNP-3, equal ratio of MUC1 and α-GalCer, and PBS were subcutaneously injected on days 7, 11 and 15, respectively. Tumor size was measured every 2 days. The mice were euthanized when the tumor length exceeded 15 mm. Tumor volume was calculated as 0.5 × length × $width^2$. After completion of the experiment on day 22, all mice were euthanized.

Results and Discussion

Synthesis and Characterization of α-GalCer-AuNP-MUC1 Vaccines

To obtain the vaccines, MUC1 glycopeptide and α-GalCer were prepared. A PEGylated amide was attached to the 6-position of galactose of α-GalCer (named as 6-NH_2-α-GalCer) so that the ability to activate CD1d receptor would not be affected. The expected molecule was synthesized through nine steps with a yield of 15% (Scheme 1). The products were confirmed by ^1H and ^{13}C NMR spectra (Figure S5-S11).

Full-length MUC1 VNTR domain with α-GalNAc modified on the Thr residue of PDTRP motif (named as MUC1(Tn)) was used as the antigen and synthesized through the strategy of solid-phase peptide synthesis (Scheme S1). Then, MUC1(Tn) was characterized by HPLC and ESI-MS (Scheme S2).

For the multivalent presentation of the MUC1 glycopeptide and α-GalCer glycolipid, AuNPs were used as the

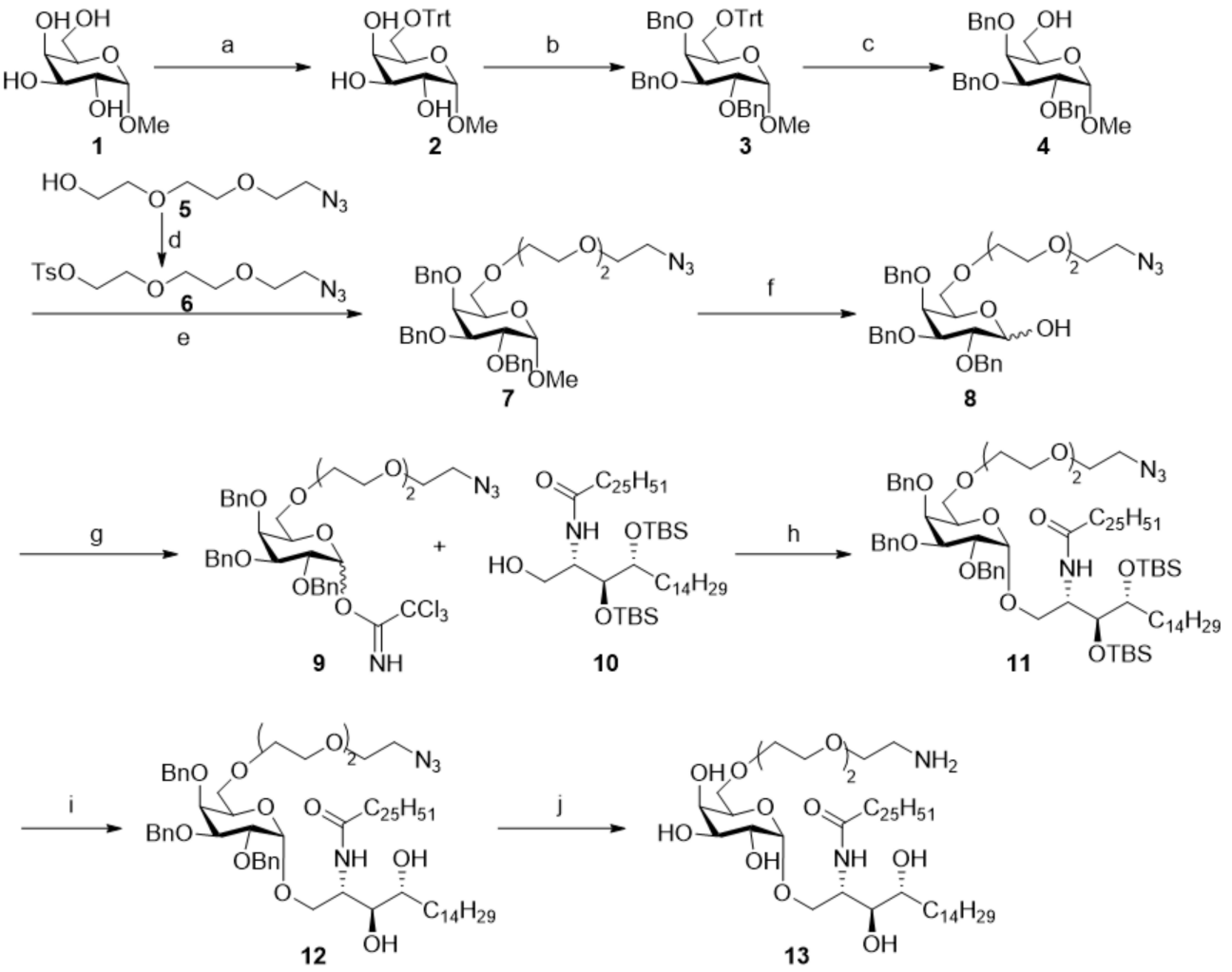

Scheme 1 The synthesis of 6-NH_2-α-GalCer (13)[a].
Notes: [a]Reagents and conditions: (a) TrtCl, pyridine, 92%; (b) NaH, BnBr, DMF; (c) *p*-TsOH, CH_2Cl_2/MeOH (1:2, v/v), 80% HOAc, 86% over two steps; (d) TsCl, pyridine, 85%; (e) NaH, DMF, 72%; (f) 0.5 M H_2SO_4/HOAc (1:8, v/v); (g) CCl_3CN, DBU, CH_2Cl_2; (h) BF_3 Et_2O, THF/Et_2O (1:5, v/v), 37% over three steps; (i) TBAF, THF, 85%; (j) Pd $(OH)_2$/C (20% w/w), H_2, EtOH/$CHCl_3$ (4:1, v/v), 83%.

nanocarriers.[44,45] We used a preparation strategy reported by Schlecht et al for the loading.[43] As shown in Scheme 2, the first two steps were carried out according to the previous report,[43] followed by coupling MUC1(Tn) glycopeptide and 6-NH_2-α-GalCer (the molar ratio of these two compounds used in the construction of AuNPs were 2:1, 1:1 and 1:2, respectively) to the obtained MUDHSE AuNPs (Scheme 2). The characterization of the constructed AuNPs vaccine candidates (AuNP-1, MUC1 (Tn)/6-NH_2-α-GalCer =2:1; AuNP-2, MUC1(Tn)/6-NH_2-α-GalCer =1:1; AuNP-3, MUC1(Tn)/6-NH_2-α-GalCer =1:2) was evaluated by UV-Vis spectra, TEM measurements and dynamic light scattering (DLS) measurements. UV-Vis spectra of these AuNPs showed that the absorption peak was at 526 nm (Figure S1). The TEM images showed the average size of these AuNPs was 5.8 ± 0.8 nm (Figure S2). DLS results showed the hydrodynamic diameter was 60 nm, 130 nm and 160 nm for AuNP1-3, respectively (Figure S3). The physicochemical characteristics of the AuNPs-based vaccines are summarized in Table 1. MUC1 glycopeptide loading was determined by BCA colorimetric method (Figure S4), and the loading of 6-NH_2-α-GalCer was determined by ^{1}H NMR spectroscopy by comparison of the integrals of selected peaks of the supernatant.

The Activation of Bone Marrow-Derived Dendritic Cells (BMDCs)

Dendritic cells (DCs) are important factors of the adaptive immune response. DCs maturation is the key step to

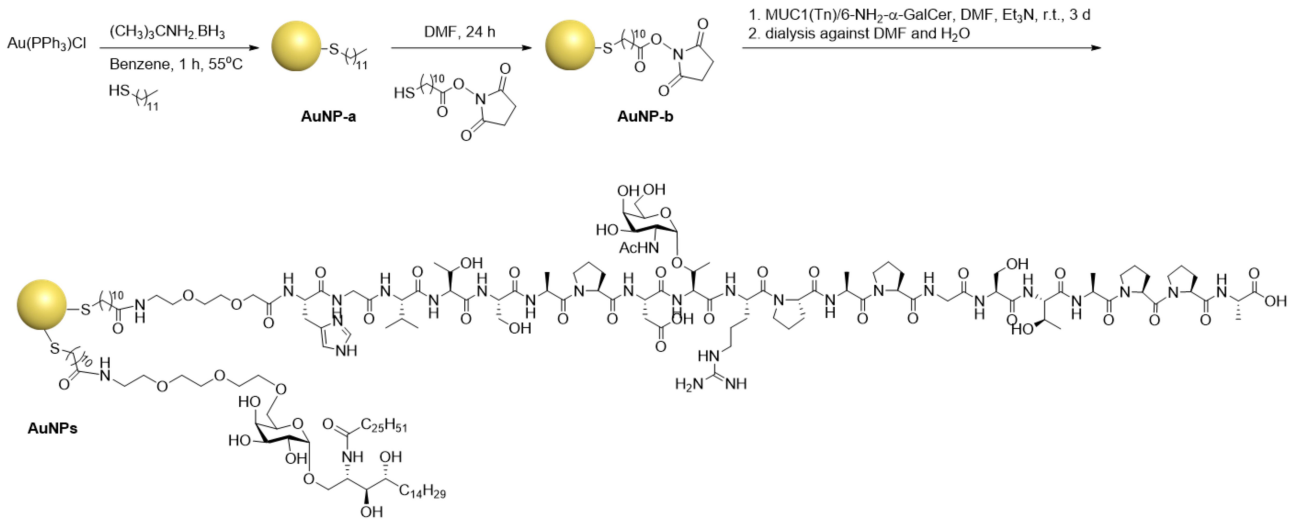

Scheme 2 Synthetic route for the preparation of AuNPs with terminally functionalized thiol nanoparticle and the immobilization of MUC1 glycopeptide and α-GalCer glycolipid.

offer costimulatory signals to T cells. To examine the ability of the prepared vaccines to induce the activation of DCs, the secretion of cytokines IL-6 and IL-12 by BMDCs exposed to the vaccine candidates was analyzed. As shown in Figure 1, AuNP-1, AuNP-2, and AuNP-3 groups induced decent production of IL-6 and IL-12, while BMDCs processed with α-GalCer+MUC1 secret only a subset. These results indicate the prepared vaccines have the potential for further immunological evaluation.

Analysis of the Antibody Titers and Subtypes

To analyze the immunological properties of these AuNP vaccine candidates, female Balb/c mice (6~8 week old, 6 mice/group) were immunized with AuNP-1, AuNP-2 and AuNP-3, PBS solution with an equal ratio of MUC1 and α-GalCer was used as the control group. The injection includes four times with an interval of 2 weeks. One week after the last immunization, sera and spleens were collected for immunological evaluation.

Table 1 The Physicochemical Characteristics of the AuNPs-Based Vaccines

AuNPs	DLS		ZP
	Ø (nm)	PDI	(mV)
AuNP-1	60 ± 7	0.20	−11
AuNP-2	130 ± 19	0.29	−22
AuNP-3	160 ± 17	0.37	−17

The antibody titers were detected by enzyme-linked immunosorbent assay (ELISA). Compared with mice injected with MUC1(Tn) and α-GalCer mixture, the three AuNP-based vaccines elicited antibody with higher titers. Among the three groups of AuNPs vaccine candidates, AuNP-1 immunization generated the highest antibody titers, while AuNP-3 is the lowest immunogenic (Figure 2). It demonstrated that the antibody titers were related to the ratio of MUC1 antigen to the α-GalCer adjuvant.

Then, we measured the concentration of different IgG subtypes (IgG1, IgG2a, IgG2b, IgG3) in each group (Figure 3). The results showed that the produced IgG were mainly IgG1 and IgG2a. Since the subtype switch to IgG1 was induced by IL-4, and IgG2a was caused by IFN-γ, the production of considerable IgG1 and IgG2a indicates a combined Th1 and Th2 response. As shown in Figure 3A–D, AuNP-based vaccines elicited MUC1-specific IgG subclasses, while the mixture of MUC1(Tn) and α-GalCer hardly induced such response. This is consistent with previous IgG results. As the ratio of IgG2a/IgG1 is associated with the balance of Th1/Th2 cell responses, and the ratio >1 indicating a Th1 response.[29] As shown in Figure 3E, AuNP-based vaccines AuNP-1, AuNP-2 and AuNP-3 induced Th1 response while α-GalCer+MUC1 induced Th2 response. Moreover, AuNP-based vaccine AuNP-1 generated higher titers than the other groups.

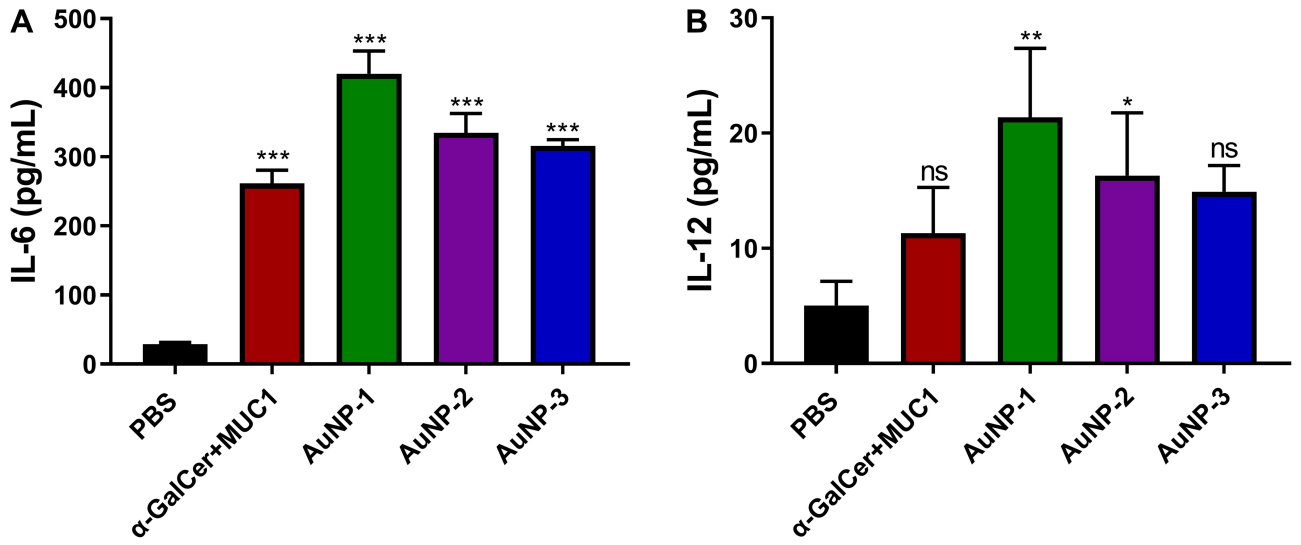

Figure 1 Proinflammatory cytokines of (**A**) IL-6 and (**B**) IL-12 were detected in the culture supernatants of mouse bone marrow-derived dendritic cells (BMDCs) exposed to PBS, α-GalCer+MUC1, AuNP-1, AuNP-2 and AuNP-3 for 18 h. Data are shown as mean ± SD. Differences among groups are determined by one-way ANOVA analysis, ns = not significant,*$p < 0.05$, **$p < 0.01$, ***$p < 0.001$.

Analysis of the Binding Capacity of the Antisera with Tumor Cells

In order to evaluate the binding affinity of the antisera with cancer cells, we performed immunofluorescence assay with MUC1-expressed human breast cancer MCF-7 cells as model cancer cells, and SK-MEL-28 cells as negative control. As shown in Figure 4, antisera induced by the vaccine candidates displayed considerable binding with MCF-7 cells, in which AuNP-1 showed the strongest binding, while MUC1 and α-GalCer mixture elicited the lowest binding. As to SK-MEL-28 cells, the antisera exhibited little binding, indicating a good specificity.

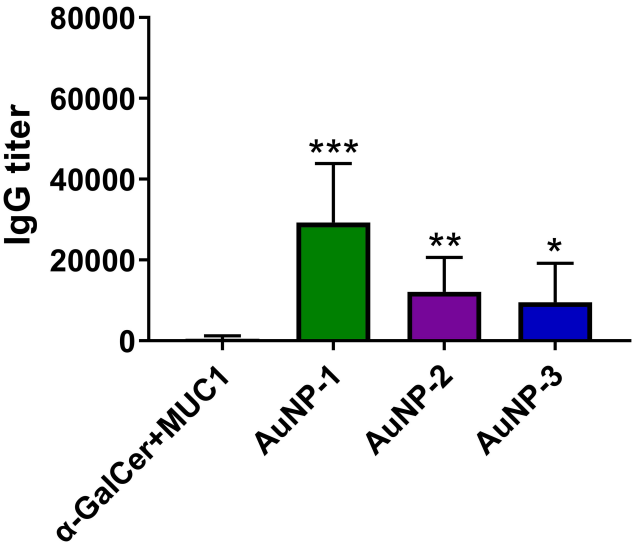

Figure 2 The antibody titers of IgG of antisera induced by the vaccine candidates were evaluated. The plates were coated with MUC1(Tn), and pre-immune sera were used as negative control. Data are shown as mean ± SD. Differences among groups are determined by one-way ANOVA analysis, *$p< 0.05$, **$p< 0.01$, and ***$p< 0.001$.

The binding capacity of the antisera elicited by these vaccine candidates with cancer cells was detected further by flow cytometry (FACS). MCF-7 cell was employed as a model cell, while SK-MEL-28 cell that does not express MUC1 antigen was served as negative control. The antisera provoked by the vaccine candidates were incubated with the two cell lines individually, followed by culturing with FITC-labeled goat anti-mouse IgG. Antisera from mice immunized with AuNP-based vaccines exhibited considerable binding with MCF-7 cells (Figure 5A), while little binding with SK-MEL-28 cells (Figure 5B). This indicated that antibodies elicited by these vaccine candidates could specifically bind with MUC1 expressing cancer cells. Moreover, the antisera elicited by AuNP-based vaccines had a stronger interaction with the MCF-7 cells than the mixture of MUC1 and α-GalCer (Figure 5A). Among the three nanovaccine groups, antisera induced by AuNP-1 vaccine presented the highest binding with the MCF-7 cells (Figure 5A).

Analysis of the Complement-Dependent Cytotoxicity (CDC) Effect of the Antisera

The anticancer activities induced by the antibodies provoked by the vaccine candidates were then analyzed by CDC. As demonstrated in Figure 6A, the cytotoxicity to MCF-7 cells induced by antisera of AuNP-based vaccines was stronger than the mixture of MUC1 and α-GalCer.

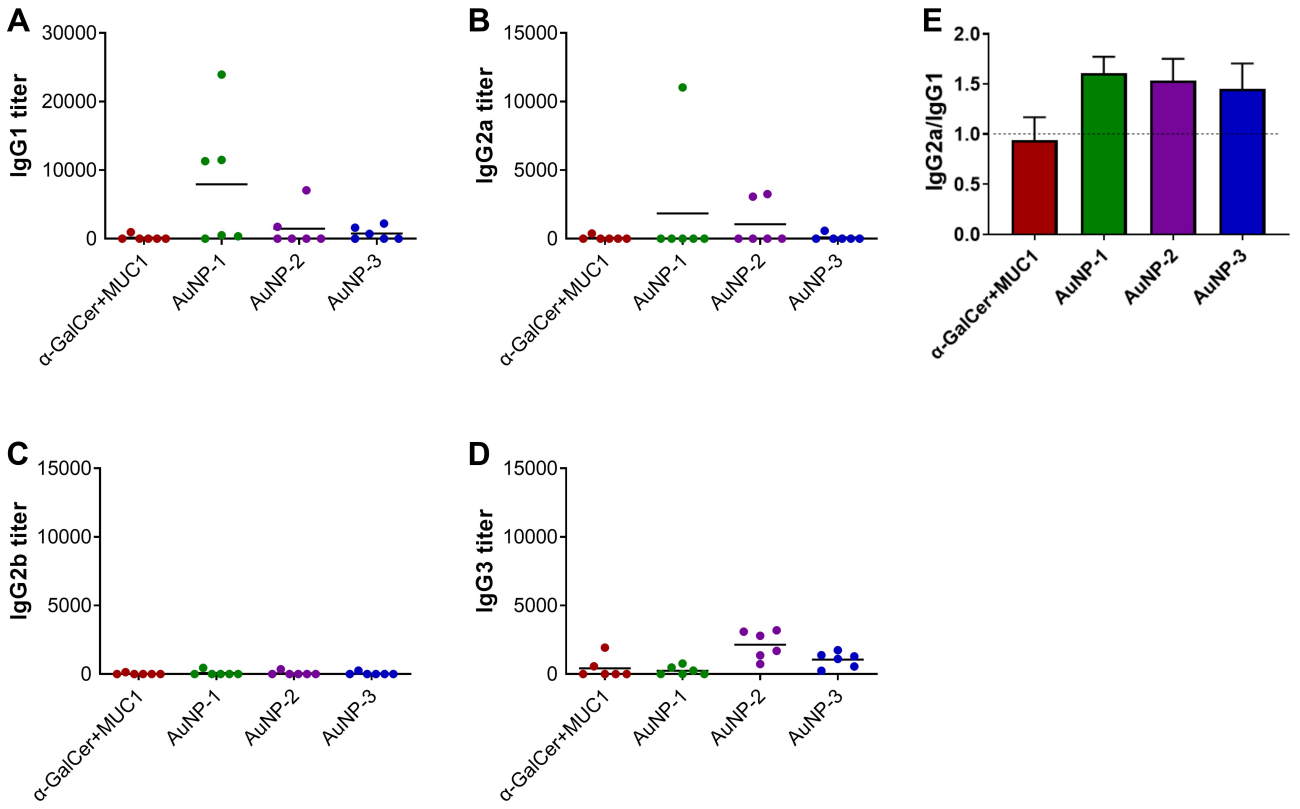

Figure 3 The titers of antibody isotypes (**A**) IgG1, (**B**) IgG2a, (**C**) IgG2b and (**D**) IgG3 of antisera induced by the vaccine candidates. The plates were coated with MUC1 (Tn), using pre-immune sera as negative control. Each dot means the result of one mouse and the horizontal bar means the average antibody titer of each group. (**E**) The ratio of IgG2a/IgG1 determined by the OD value at a dilution of 1:1000. Data are shown as mean ± SD.

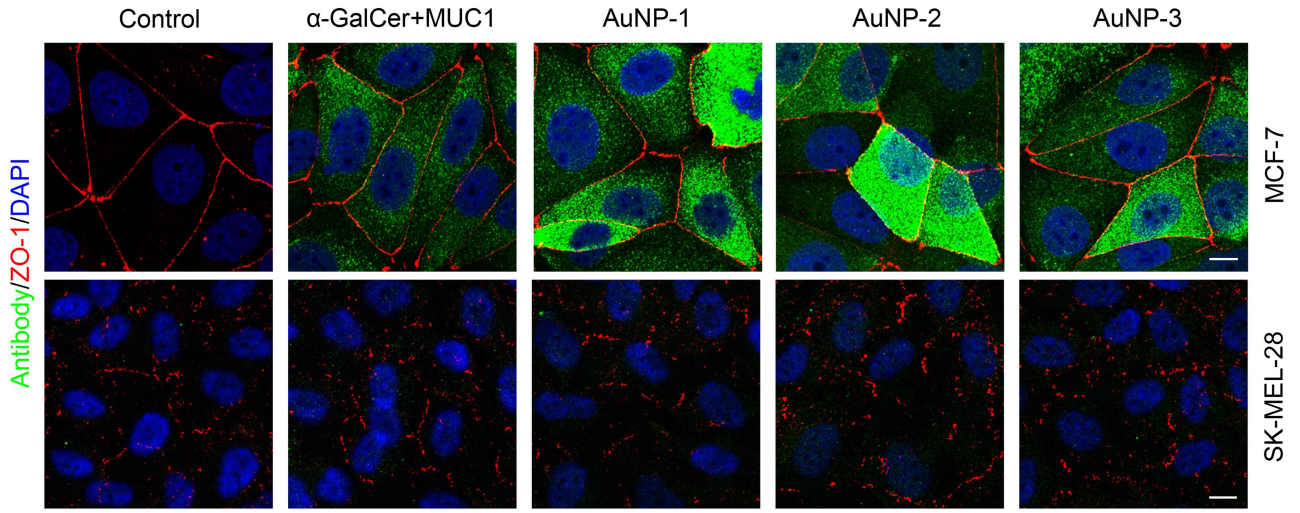

Figure 4 Immunofluorescence of MCF cells and SK-MEL-28 cells. The cells were fixed, permeabilized and then incubated with 1:50 dilution of antisera from different groups (MUC1(Tn)+α-GalCer, AuNP-1, AuNP-2, AuNP-3). FITC-labeled anti-mouse IgG (green) was employed to label the antisera. The sera from PBS immuned mice were employed as control. DAPI was employed to stain cell nucleus (blue). ZO-1 was employed to stain cell membrane (red). The scale bar was 10 μm.

The lysis rates of MCF-7 cells induced by the antisera of AuNP-1, AuNP-2 and AuNP-3 were about 54%, 44% and 29%, respectively. However, there was almost no CDC to SK-MEL-28 cells (Figure 6B). This indicated the antisera induced by the vaccine candidates mediated specific CDC to the cancer cells that express MUC1 antigen. The results were in good agreement with the binding activities of the antisera with cancer cells in the experiments above.

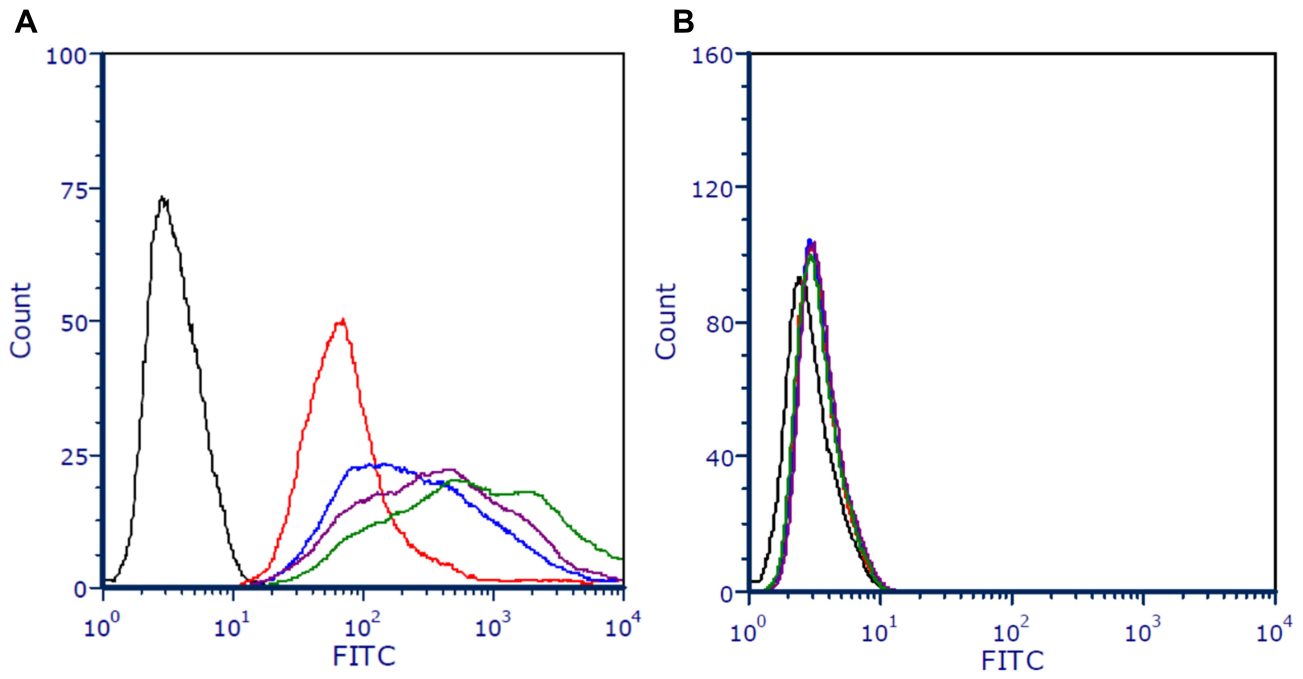

Figure 5 FACS evaluation of the antisera binding with MCF-7 cells (**A**) and SK-MEL-28 cells (**B**). One representative result of the FACS evaluation is shown for each group of vaccine candidates. The antisera from vaccine candidates AuNP-1 (green), AuNP-2 (purple), AuNP-3 (blue), α-GalCer+MUC1 (red). The sera from PBS immunized mice were employed as control (black).

Analysis of the Cytokines Secretion of the Splenocytes

The cytokine levels secreted by splenocytes were then detected after immunization. The collected splenocytes were retreated with MUC1, and the expression levels of IL-4 and IFN-γ were analyzed by ELISA kit. IL-4, a kind of Th2-type cytokines, can promote the maturation of B cells and antibody switching to IgG1; IFN-γ, a kind of Th1-type cytokines generated by $CD8^+$ cytotoxic T cells or Th1 cells, can activate macrophages to switch antibody to be IgG2a. As shown in Figure 7A, splenocytes from mice injected with AuNP-based vaccines secreted higher levels of IL-4 than the control group. Moreover, among the AuNP-based vaccine candidates, the IL-4 level of AuNP-1 group was higher than those in AuNP-2 and AuNP-3

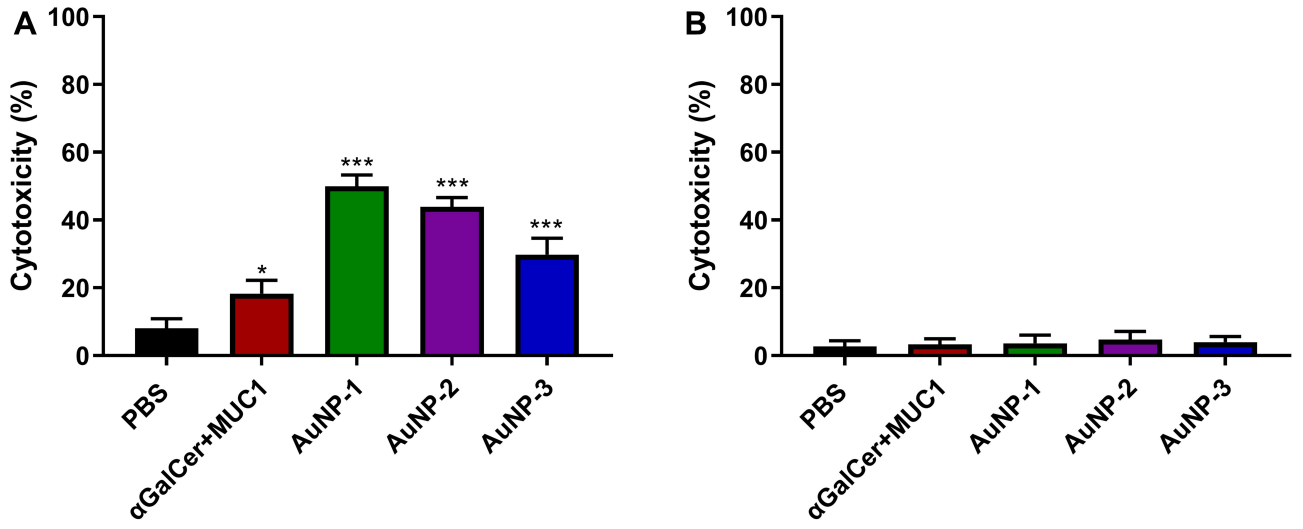

Figure 6 Complement dependent cytotoxicity to MCF-7 cells (**A**) and SK-MEL-28 cells (**B**) elicited by the sera collected from the mice immunized with the vaccines. Data are shown as mean ± SD. Differences among groups are determined by one-way ANOVA analysis, $*p < 0.05$, $***p < 0.001$.

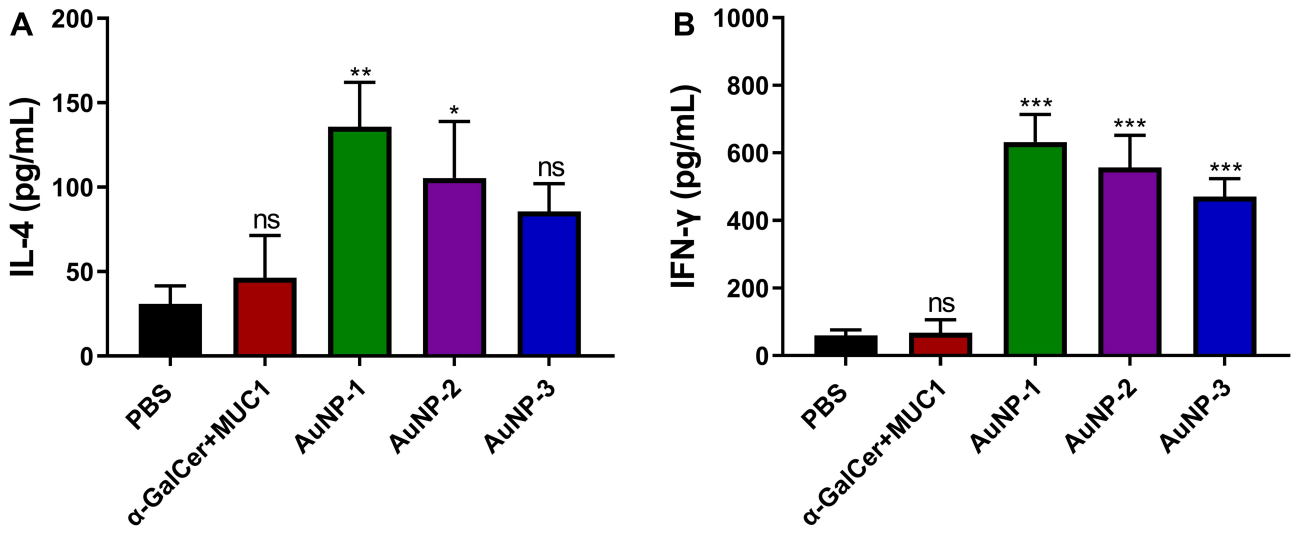

Figure 7 The splenocytes were isolated from immunized mice and retreated with MUC1 glycopeptide, then the secretion of (**A**) IL-4 and (**B**) IFN-γ in culture supernatants were analyzed by ELISA kit. Data are shown as mean ± SD. Differences among groups are determined by one-way ANOVA analysis, ns = not significant, *$p < 0.05$, **$p < 0.01$, ***$p < 0.001$.

groups. Similar results were discovered in the assessment of IFN-γ level (Figure 7B). It is worth noting that, compared with AuNPs conjugate vaccine groups, little IL-4 and IFN-γ were detected in the group of α-GalCer + MUC1, which may be attributed to the anergy of NKT cells.[46,47] In general, these results showed that AuNP-based vaccine candidates induced IL-4 and IFN-γ, indicating a mixed Th1/Th2 response. This phenomenon is in agreement with previous results of antibody subtypes.

Analysis of the Ratio of $CD8^+$ T Cells and in vitro CTL Assay

T cell-mediated specific immune response is essential to the process of tumor progression, in which $CD8^+$ T lymphocytes can target the tumor cells and kill them. Therefore, the ratio of $CD8^+$ T cells was first examined. Briefly, splenocytes were collected and stained by CD3 and CD8 antibodies to identify the $CD3^+CD8^+$ T cells. As shown in Figure 8, a significant expansion of $CD3^+CD8^+$ T cells was observed in the spleens of mice vaccinated by the AuNP-1, AuNP-2 and AuNP-3. The result indicated the vaccines could increase the ratio of $CD3^+CD8^+$ T cells, which might lead to antigen-specific cytotoxicity of cytotoxic T lymphocytes for tumor suppression.

Then, MUC1-specific cytotoxicity of cytotoxic T lymphocytes (CTL) was measured. The spleens were harvested from mice immunized with the vaccine candidates. Then, splenocytes were isolated and added to 1×10^5 MCF-7 cells or SK-MEL-28 cells with a ratio of 50:1. The viabilities of the tumor cells were detected after co-incubation. The result indicated the mixture of MUC1 and α-GalCer was ineffective to induce antitumor CTL responses. While AuNP-based vaccines, especially AuNP-1, showed significant lysis of MCF-7 cells (Figure 9A). However, only few CTL effect was elicited by all the vaccine candidates to SK-MEL-28 cells (Figure 9B), this might be due to the fact that the induced CTL responses were mainly MUC1 specific.

Therapeutic Antitumor Effect of α-GalCer-AuNP-MUC1 Vaccines in B16-MUC1 Melanoma Tumor Model

Finally, the in vivo therapeutic efficiency of the vaccine candidates was examined. B16-MUC1 tumor cells (1×10^5) were subcutaneously inoculated on female C57BL/6 mice. Vaccination was then performed every 4 days for three times 1 week later. The tumor growth curves in Figure 10 showed that AuNP-based vaccines had better inhibition on tumor growth than the control group. Among the AuNP-based vaccines, AuNP-1 significantly delayed the tumor growth. These results indicated that antigens and immune adjuvants conjugation on AuNP could enhance the cancer immunotherapy. And the molar ratio of antigens and adjuvants showed a positive correlation with in vivo tumor-suppressive activity. Moreover, there was no obvious change in the body weight of the mice, which indicated the vaccine candidates were biologically safe without obvious toxicity.

The infiltration of effector $CD8^+$ T cells into tumor tissue was vital for cancer vaccines, as tumor-infiltrating

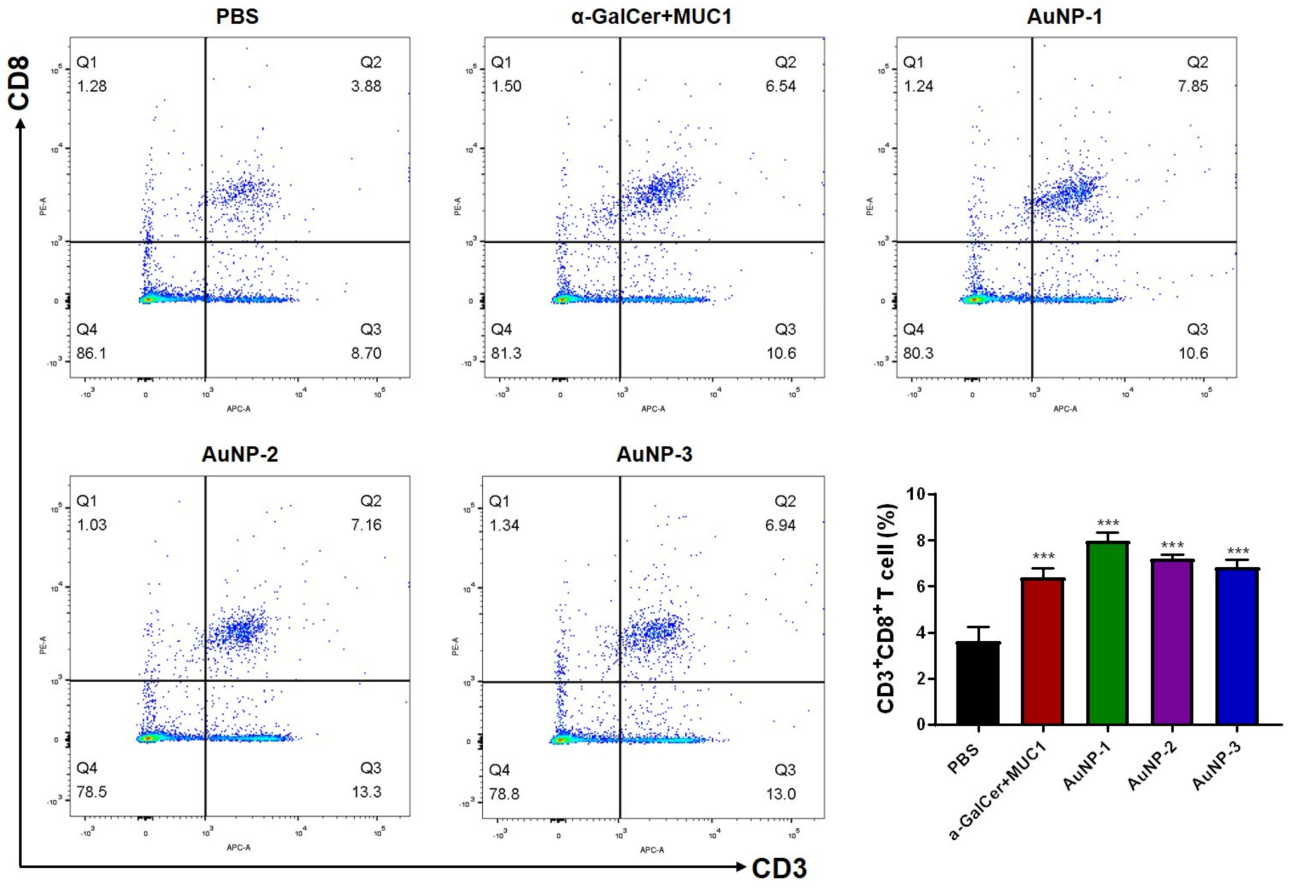

Figure 8 Ratio of $CD8^+$ T cells isolated from the spleens of the mice immunized with the vaccine candidates. Data are shown as mean ± SD (n = 3). Differences among groups are determined by one-way ANOVA analysis. ***$p < 0.001$.

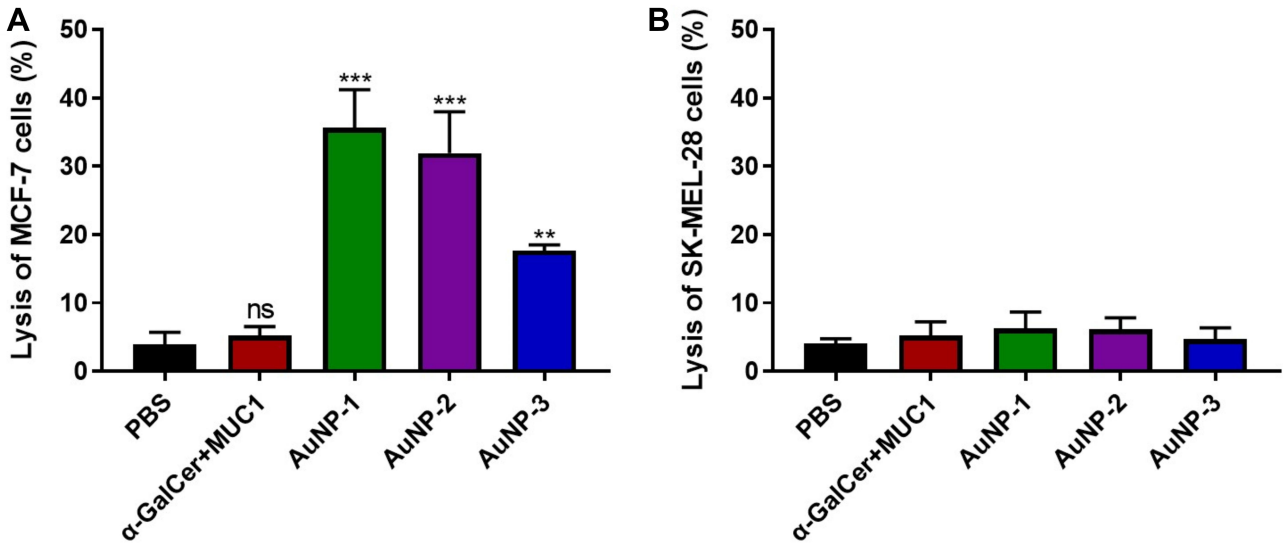

Figure 9 MUC1-specific CTL cytotoxicity elicited by the vaccine candidates to (**A**) MCF-7 cells and (**B**) SK-MEL-28 cells. The ratio of splenocytes to MCF-7 cells or SK-MEL-28 cells was 50:1. Data are shown as mean ± SD. Differences among groups are determined by one-way ANOVA analysis. ns = not significant, **$p < 0.01$, ***$p < 0.001$.

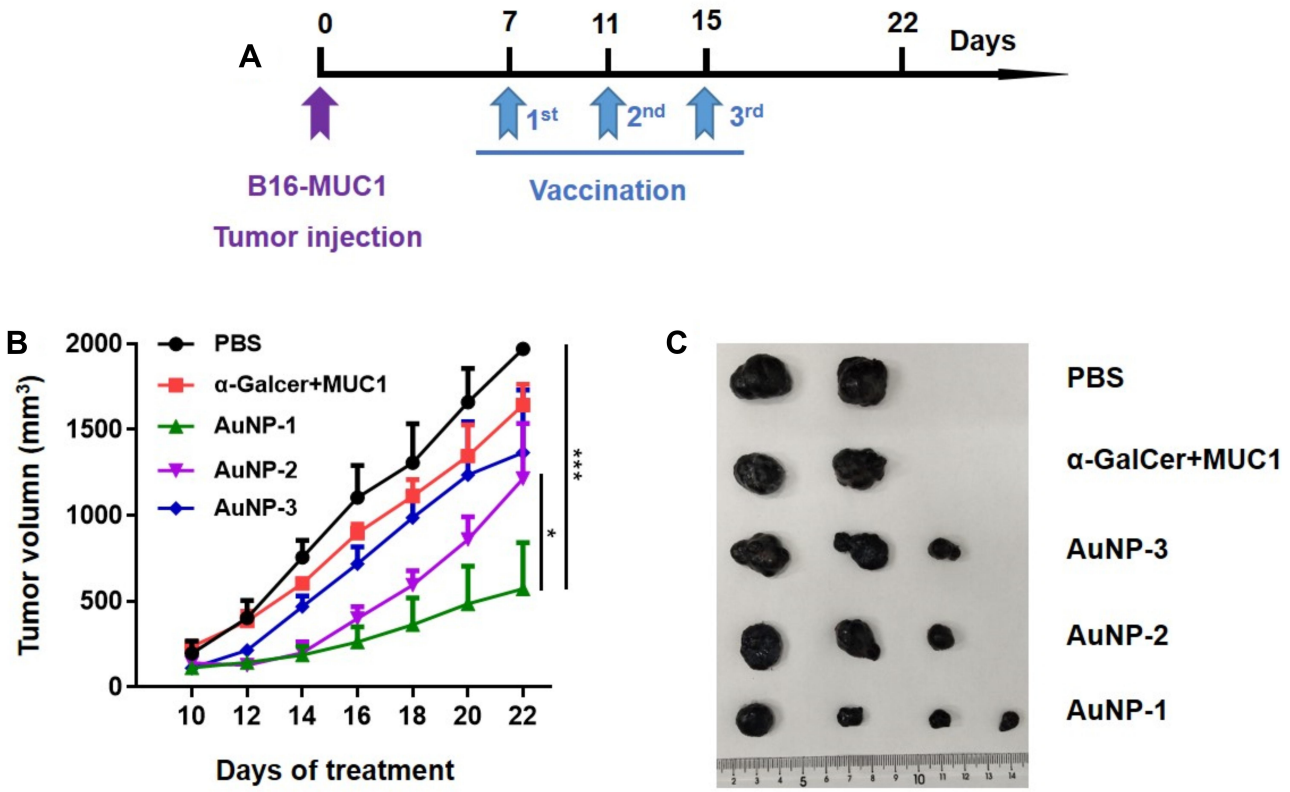

Figure 10 Therapeutic immune activities of the vaccine candidates against melanoma. (**A**) Scheme of the treatments in B16-MUC1 tumor model. Female C57BL/6 Mice were subcutaneously challenged with B16-MUC1 melanoma cells on day 0. The vaccine candidates were injected on day 7, day 11 and day 15. (**B**) Mean tumor growth curves presented by volume of tumors. Data are shown as mean ± SD (n = 5). Differences among groups are determined by two-way ANOVA analysis, *$p < 0.05$, ***$p < 0.001$. (**C**) Photos of tumors excised at day 22.

$CD8^+$ T cells would release granzymes or perforin to eliminate tumor cells. The final antitumor effect was largely depended on the activity of tumor-infiltrating $CD8^+$ T lymphocytes. As shown in Figure 11, vaccination of AuNP-based vaccines, especially AuNP-1 effectively improved the infiltration of effector $CD8^+$ T lymphocytes into tumor tissue. These results further suggested AuNP-based vaccines, especially AuNP-1 could magnify the tumor-infiltrating of activated $CD8^+$ T cells.

In this work, we have synthesized multivalent gold nanoparticle vaccines conjugated with MUC1 glycopeptide antigen and α-GalCer adjuvant. Compared with previous α-GalCer adjuvant vaccines that employed carbohydrates or peptides as B cell epitopes,[28,31] glycopeptide was applied in this study, which would provide important information to study the immune mechanism of the vaccines. Moreover, α-GalCer adjuvant was usually coupled with antigens by a chemical bond,[26,28,31,32] which is difficult to perform the covalent reaction between hydrophobic α-GalCer with hydrophilic antigens. The proposed multiple carrier of AuNPs allowed facile incorporation of α-GalCer with various kinds of antigens. Compared with the mixture of MUC1(Tn) antigen and α-GalCer adjuvant, their covalent conjugate through AuNPs elicited more powerful immune responses. From the immunological evaluation results, the immune efficiency of AuNP-1 was superior to AuNP-2 and AuNP-3. One possible reason was that the diameter of AuNP-1 was <100 nm, since the particles of 10–100 nm can move more efficiently from interstitium to lymphatic capillaries, then transfer to lymph nodes for the uptake by APCs.[48] Another reason was that NKT cell anergy might be induced when a larger amount of α-GalCer was administrated. From the immunological results, we observed that in the constructed vaccines of AuNP-1 (4.5 nmol α-GalCer), AuNP-2 (9 nmol α-GalCer) and AuNP-3 (18 nmol α-GalCer), as the dose of α-GalCer increases, the immune efficacy of the vaccines gradually decreased. The results were consistent with previously reported NKT cell anergy.[46,47] What is more, for the AuNP-based vaccines, the antitumor humoral and cellular immune responses were found to be positively correlated with the molar

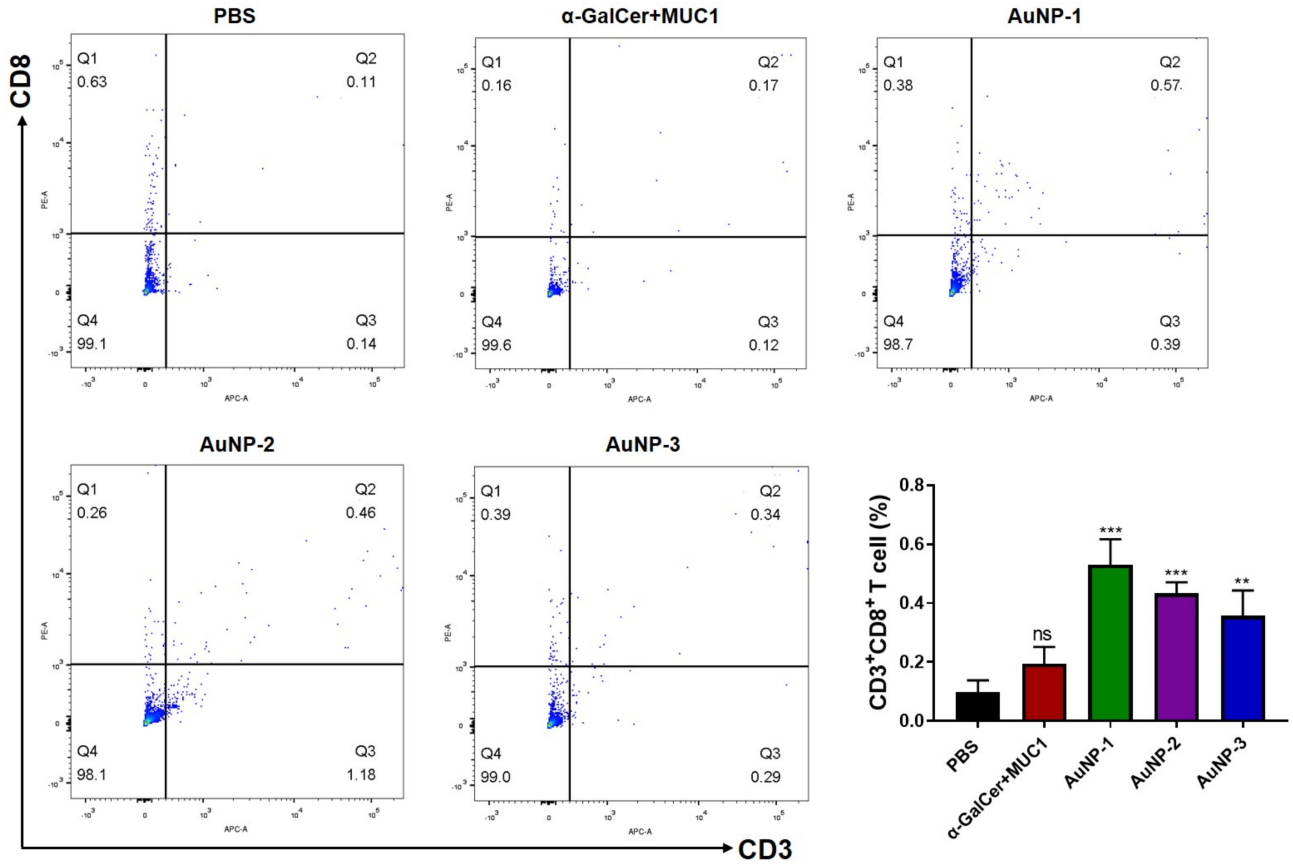

Figure 11 The infiltration of $CD8^+$ T cells in tumor. Female C57BL/6 Mice were subcutaneously challenged with B16-MUC1 melanoma cells on day 0. The vaccine candidates were injected on day 7, day 11 and day 15. The mice were sacrificed on day 21 and tumor were collected to analyze the infiltration of $CD8^+$ T cells. Data are shown as mean ± SD (n = 3). Differences among groups are determined by one-way ANOVA analysis. ns = not significant, $^{**}p < 0.01$, $^{***}p < 0.001$.

ratio of MUC1(Tn) glycopeptide antigen to α-GalCer adjuvant, which need further research.

Conclusions

In conclusion, novel MUC1 glycopeptide-based cancer vaccine candidates were constructed, with α-GalCer as the adjuvant and gold nanoparticle as a multivalent carrier. Immunological evaluation showed that these vaccine candidates elicited decent antibody titers. The binding affinity experiment of both FACS analysis and immunofluorescence assay demonstrated that the induced antisera showed strong binding with MUC1 positive MCF-7 cells, while little binding with the MUC1 negative SK-MEL-28 cells. Moreover, the produced antibody can mediate CDC to kill MCF-7 cells. Besides stimulating B cells to generate MUC1-specific antibodies, the prepared vaccines also stimulated in vitro MUC1-specific CTLs. Finally, the vaccines significantly inhibited tumor growth in the therapeutic tumor model. The good ability to stimulate both humoral and cellular immune responses indicated the tremendous potential of the strategy of conjugating antigen and α-galactosylceramide (α-GalCer) adjuvant with multivalent carrier of gold nanoparticles in the treatment of cancer and other diseases such as virus or bacterial infections.

Abbreviations

MUC1, Mucin 1; α-GalCer, α-galactosylceramide; TACA, tumor-associated carbohydrate antigen; AuNPs, Gold nanoparticles; BSA, bovine serum albumin; KLH, keyhole limpet hemocyanin; TTX, tetanus toxoid; CDC, complement-dependent cytotoxicity; CTL, cytotoxic T lymphocytes; TLR, Toll-like receptor; APC, antigen-presenting cell.

Acknowledgments

This work was supported by the National Natural Science Foundation of China (22077068), the National Key R&D Program of China (Grant No. 2018YFA0507204), the NCC Fund (NCC2020FH12), the Natural Science Foundation of

Tianjin (19JCQNJC05300) and the Fundamental Research Funds for the Central Universities.

Disclosure

The authors declare no competing financial interests.

References

1. Melief CJ, van Hall T, Arens R, Ossendorp F, van der Burg SH. Therapeutic cancer vaccines. *J Clin Invest*. 2015;125(9):3401–3412. doi:10.1172/JCI80009
2. Mukherjee P, Madsen CS, Ginardi AR, et al. Mucin 1-specific immunotherapy in a mouse model of spontaneous breast cancer. *J Immunother (1991)*. 2003;26(1):47–62. doi:10.1097/00002371-200301000-00006
3. Taylor-Papadimitriou J, Burchell J, Miles DW, Dalziel M. MUC1 and cancer. *BBA-Mol Basis Dis*. 1999;1455(2–3):301–313. doi:10.1016/S0925-4439(99)00055-1
4. Tang CK, Katsara M, Apostolopoulos V. Strategies used for MUC1 immunotherapy: human clinical studies. *Expert Rev Vaccines*. 2008;7(7):963–975. doi:10.1586/14760584.7.7.963
5. Gaidzik N, Westerlind U, Kunz H. The development of synthetic antitumour vaccines from mucin glycopeptide antigens. *Chem Soc Rev*. 2013;42(10):4421–4442. doi:10.1039/c3cs35470a
6. Deguchi T, Tanemura M, Miyoshi E, et al. Increased immunogenicity of tumor-associated antigen, mucin 1, engineered to express alpha-gal epitopes: a novel approach to immunotherapy in pancreatic cancer. *Cancer Res*. 2010;70(13):5259–5269. doi:10.1158/0008-5472.CAN-09-4313
7. Cai H, Huang Z-H, Shi L, et al. Variation of the glycosylation pattern in MUC1 glycopeptide BSA vaccines and its influence on the immune response. *Angew Chem Int Edit*. 2012;51(7):1719–1723. doi:10.1002/anie.201106396
8. Zhu J, Wan Q, Lee D, et al. From synthesis to biologics: preclinical data on a chemistry derived anticancer vaccine. *J Am Chem Soc*. 2009;131(26):9298–9303. doi:10.1021/ja901415s
9. Kaiser A, Gaidzik N, Westerlind U, et al. A synthetic vaccine consisting of a tumor-associated Sialyl-TN-MUC1 tandem-repeat glycopeptide and tetanus toxoid: induction of a strong and highly selective immune response. *Angew Chem Int Edit*. 2009;48(41):7551–7555. doi:10.1002/anie.200902564
10. Ingale S, Wolfert MA, Gaekwad J, Buskas T, Boons GJ. Robust immune responses elicited by a fully synthetic three-component vaccine. *Nat Chem Biol*. 2007;3(10):663–667. doi:10.1038/nchembio.2007.25
11. Wilkinson BL, Day S, Malins LR, Apostolopoulos V, Payne RJ. Self-adjuvanting multicomponent cancer vaccine candidates combining per-glycosylated MUC1 glycopeptides and the toll-like receptor 2 agonist Pam3CysSer. *Angew Chem Int Edit*. 2011;123(7):1673–1677. doi:10.1002/ange.201006115
12. Hartmann S, Nuhn L, Palitzsch B, et al. CpG-loaded multifunctional cationic nanohydrogel particles as self-adjuvanting glycopeptide antitumor vaccines. *Adv Healthc Mater*. 2015;4(4):522–527. doi:10.1002/adhm.201400460
13. McDonald DM, Wilkinson BL, Corcilius L, Thaysen-Andersen M, Byrne SN, Payne RJ. Synthesis and immunological evaluation of self-adjuvanting MUC1-macrophage activating lipopeptide 2 conjugate vaccine candidates. *Chem Commun*. 2014;50(71):10273–10276. doi:10.1039/C4CC03510K
14. Liu Y, Zhang W, He Q, et al. Fully synthetic self-adjuvanting MUC1-fibroblast stimulating lipopeptide 1 conjugates as potential cancer vaccines. *Chem Commun*. 2016;52(72):10886–10889. doi:10.1039/C6CC04623A
15. Zhou ZF, Mondal M, Liao GC, Guo ZW. Synthesis and evaluation of monophosphoryl lipid A derivatives as fully synthetic self-adjuvanting glycoconjugate cancer vaccine carriers. *Org Biomol Chem*. 2014;12(20):3238–3245. doi:10.1039/C4OB00390J
16. Huang ZH, Shi L, Ma JW, et al. A totally synthetic, self-assembling, adjuvant-free MUC1 glycopeptide vaccine for cancer therapy. *J Am Chem Soc*. 2012;134(21):8730–8733. doi:10.1021/ja211725s
17. Liu Y, Wang Y, Yu F, et al. Potentiating the immune response of MUC1-based antitumor vaccines using a peptide-based nanovector as a promising vaccine adjuvant. *Chem Commun*. 2017;53(68):9486–9489. doi:10.1039/C7CC04386D
18. Crowe NY, Coquet JM, Berzins SP, et al. Differential antitumor immunity mediated by NKT cell subsets in vivo. *J Exp Med*. 2005;202(9):1279–1288. doi:10.1084/jem.20050953
19. Carreno LJ, Kharkwal SS, Porcelli SA. Optimizing NKT cell ligands as vaccine adjuvants. *Immunotherapy*. 2014;6(3):309–320. doi:10.2217/imt.13.175
20. Taniguchi M, Harada M, Kojo S, Nakayama T, Wakao H. The regulatory role of Vα14 NKT cells in innate and acquired immune response. *Annu Rev Immunol*. 2003;21(1):483–513. doi:10.1146/annurev.immunol.21.120601.141057
21. Godfrey DI, Kronenberg M. Going both ways: immune regulation via CD1d-dependent NKT cells. *J Clin Invest*. 2004;114(10):1379–1388. doi:10.1172/JCI200423594
22. Bendelac A, Savage PB, Teyton L. The biology of NKT cells. *Annu Rev Immunol*. 2007;25(1):297–336. doi:10.1146/annurev.immunol.25.022106.141711
23. Tyznik AJ, Tupin E, Nagarajan NA, Her MJ, Benedict CA, Kronenberg M. Cutting edge: the mechanism of invariant NKT cell responses to viral danger signals. *J Immunol*. 2008;181(7):4452–4456. doi:10.4049/jimmunol.181.7.4452
24. Hayakawa Y, Rovero S, Forni G, Smyth MJ. Alpha-galactosylceramide (KRN7000) suppression of chemical- and oncogene-dependent carcinogenesis. *Proc Natl Acad Sci U S A*. 2003;100(16):9464–9469. doi:10.1073/pnas.1630663100
25. Yang G, Schmieg J, Tsuji M, Franck RW. The C-glycoside analogue of the immunostimulant alpha-galactosylceramide (KRN7000): synthesis and striking enhancement of activity. *Angew Chem Int Edit*. 2004;43(29):3818–3822. doi:10.1002/anie.200454215
26. Bai L, Deng S, Reboulet R, et al. Natural killer T (NKT)-B-cell interactions promote prolonged antibody responses and long-term memory to pneumococcal capsular polysaccharides. *Proc Natl Acad Sci U S A*. 2013;110(40):16097–16102. doi:10.1073/pnas.1303218110
27. Deng S, Bai L, Reboulet R, et al. A peptide-free, liposome-based oligosaccharide vaccine, adjuvanted with a natural killer T cell antigen, generates robust antibody responses in vivo. *Chem Sci*. 2014;5(4):1437–1441. doi:10.1039/C3SC53471E
28. Cavallari M, Stallforth P, Kalinichenko A, et al. A semisynthetic carbohydrate-lipid vaccine that protects against S. pneumoniae in mice. *Nat Chem Biol*. 2014;10(11):950–956. doi:10.1038/nchembio.1650
29. Bessa J, Kopf M, Bachmann MF. Cutting edge: IL-21 and TLR signaling regulate germinal center responses in a B cell-intrinsic manner. *J Immunol*. 2010;184(9):4615–4619. doi:10.4049/jimmunol.0903949
30. Broecker F, Gotze S, Hudon J, et al. Synthesis, liposomal formulation, and immunological evaluation of a minimalistic carbohydrate-alpha-GalCer vaccine candidate, J. *Med Chem*. 2018;61(11):4918–4927. doi:10.1021/acs.jmedchem.8b00312
31. Anderson RJ, Tang CW, Daniels NJ, et al. A self-adjuvanting vaccine induces cytotoxic T lymphocytes that suppress allergy. *Nat Chem Biol*. 2014;10(11):943–949. doi:10.1038/nchembio.1640
32. Anderson RJ, Compton BJ, Tang CW, et al. NKT cell-dependent glycolipid-peptide vaccines with potent anti-tumour activity. *Chem Sci*. 2015;6(9):5120–5127. doi:10.1039/C4SC03599B

33. Compton BJ, Tang CW, Johnston KA, et al. Synthesis and activity of 6′′-Deoxy-6′′-thio-alpha-GalCer and peptide conjugates. *Org Lett*. 2015;17(24):5954–5957. doi:10.1021/acs.orglett.5b02836
34. Chen XZ, Zhang RY, Wang XF, et al. Peptide-free synthetic nicotine vaccine candidates with alpha-Galactosylceramide as adjuvant. *Mol Pharm*. 2019;16(4):1467–1476. doi:10.1021/acs.molpharmaceut.8b01095
35. Lee IH, Kwon HK, An S, et al. Imageable antigen-presenting gold nanoparticle vaccines for effective cancer immunotherapy in vivo. *Angew Chem Int Edit*. 2012;51(35):8800–8805. doi:10.1002/anie.201203193
36. Brinas RP, Sundgren A, Sahoo P, et al. Design and synthesis of multifunctional gold nanoparticles bearing tumor-associated glycopeptide antigens as potential cancer vaccines. *Bioconjugate Chem*. 2012;23(8):1513–1523. doi:10.1021/bc200606s
37. Parry AL, Clemson NA, Ellis J, Bernhard SS, Davis BG, Cameron NR. 'Multicopy multivalent' glycopolymer-stabilized gold nanoparticles as potential synthetic cancer vaccines. *J Am Chem Soc*. 2013;135(25):9362–9365. doi:10.1021/ja4046857
38. Cai H, Degliangeli F, Palitzsch B, et al. Glycopeptide-functionalized gold nanoparticles for antibody induction against the tumor associated mucin-1 glycoprotein. *Bioorg Med Chem*. 2016;24(5):1132–1135. doi:10.1016/j.bmc.2016.01.044
39. Marradi M, Chiodo F, Garcia I, Penades S. Glyconanoparticles as multifunctional and multimodal carbohydrate systems. *Chem Soc Rev*. 2013;42(11):4728–4745. doi:10.1039/c2cs35420a
40. Boisselier E, Astruc D. Gold nanoparticles in nanomedicine: preparations, imaging, diagnostics, therapies and toxicity. *Chem Soc Rev*. 2009;38(6):1759–1782. doi:10.1039/b806051g
41. Companon I, Guerreiro A, Mangini V, et al. Structure-based design of potent tumor-associated antigens: modulation of peptide presentation by single-atom O/S or O/Se substitutions at the glycosidic linkage. *J Am Chem Soc*. 2019;141(9):4063–4072. doi:10.1021/jacs.8b13503
42. Qian Y, Jin H, Qiao S, et al. Targeting dendritic cells in lymph node with an antigen peptide-based nanovaccine for cancer immunotherapy. *Biomaterials*. 2016;98:171–183. doi:10.1016/j.biomaterials.2016.05.008
43. Tavernaro I, Hartmann S, Sommer L, et al. Synthesis of tumor-associated MUC1-glycopeptides and their multivalent presentation by functionalized gold colloids. *Org Biomol Chem*. 2015;13(1):81–97. doi:10.1039/C4OB01339E
44. Saha K, Agasti SS, Kim C, Li X, Rotello VM. Gold nanoparticles in chemical and biological sensing. *Chem Soc Rev*. 2012;112(5):2739–2779. doi:10.1021/cr2001178
45. Daniel MC, Astruc D. Gold nanoparticles: assembly, supramolecular chemistry, quantum-size-related properties, and applications toward biology, catalysis, and nanotechnology. *Chem Rev*. 2004;104:293–346.
46. Singh AK, Gaur P, Das SN. Natural killer T cell anergy, co-stimulatory molecules and immunotherapeutic interventions. *Hum Immunol*. 2014;75(3):250–260. doi:10.1016/j.humimm.2013.12.004
47. Parekh VV, Wilson MT, Olivares-Villagomez D, et al. Glycolipid antigen induces long-term natural killer T cell anergy in mice. *J Clin Invest*. 2005;115(9):2572–2583. doi:10.1172/JCI24762
48. Jiang H, Wang Q, Sun X. Lymph node targeting strategies to improve vaccination efficacy. *J Control Release*. 2017;267:47–56. doi:10.1016/j.jconrel.2017.08.009